NASA
Technical
Paper
2411

April 1985

Effects of Inlet Distortion on a Static Pressure Probe Mounted on the Engine Hub in an F-15 Airplane

Donald L. Hughes,
Lawrence P. Myers,
and Karen G. Mackall

NASA

NASA Technical Paper 2411

1985

Effects of Inlet Distortion on a Static Pressure Probe Mounted on the Engine Hub in an F-15 Airplane

Donald L. Hughes,
Lawrence P. Myers,
and Karen G. Mackall

Ames Research Center
Dryden Flight Research Facility
Edwards, California

NASA

National Aeronautics and Space Administration

Scientific and Technical Information Branch

SUMMARY

Flight test results of an engine inlet static pressure probe (PS2) on the hub of an F100 engine in an F-15 airplane showed that a single static pressure measurement correlated well with distortion factors for both low- and high-distortion conditions. For low-distortion conditions, the ratio of engine-face total pressure to static pressure (PT2/PS2) agreed well with previous altitude facility data. Distortion of the inlet airflow was obtained by the off-schedule operation of the inlet third ramp with constant throttle at steady-state flight conditions. Data from four separate ramp excursions which caused four engine stalls showed that the distortion for these highly disturbed flow conditions was predominantly circumferential and not radial. The PT2/PS2 pressure ratio correlated well with the circumferential distortion factor (Kθ), the fan distortion factor (KA2), and the maximum-minus-minimum-over-average distortion factor (DTMM).

INTRODUCTION

Knowledge of the pressure conditions at the engine face and the measurement techniques required to define these conditions is important for the efficient operation of an air-breathing propulsion system. A measurement of pressure at the engine face is a desirable engine control parameter, but its accurate measurement requires a steady-state rake which is complex and requires many pressure sensors. A single total pressure probe may be used, but is subject to engine-face flow distortion and may not give an accurate measurement. An alternate method of determining engine-face pressure is to measure the static pressure. Static orifices on the duct wall are subject to the same distortion influences as total pressure probes. However, a single static pressure measurement upstream of the engine hub in the stream flow has been found to provide a pressure signal suitable for engine control.

A probe for measuring static pressure (PS2) was designed for and mounted on the F100-PW-100 turbofan engine for evaluation in the NASA Lewis Research Center altitude facility (ref. 1). This same probe was then evaluated on an F-15 test aircraft in flight (ref. 2) at the NASA Ames Research Center's Dryden Flight Research Facility. The probe was also used as a static pressure sensor for a digital electronic engine control system (ref. 3).

Most of the PS2 flight data were acquired with the inlet ramps operating on their normal schedule, which resulted in low values of total pressure distortion at the engine face. In order to provide higher distortion levels, the inlet third ramp was moved to off-schedule positions. This reduced the inlet throat area and increased throat inlet Mach number and engine-face distortion until the engine stalled.

The purpose of this report is to evaluate measurements made at the engine face under conditions of distortion higher than previously reported. The data evaluation related several distortion factors to engine-face total to static pressure (PT2/PS2). Engine-face maps are presented for some of these conditions.

NOMENCLATURE

b factor	Pratt & Whitney radial distortion weighting factor
DTMM	distortion factor = (PT2MAX - PT2MIN)/PT2AVG
f	function
KA2	fan distortion factor, KA2 = Kθ + b(KRA2)
KRA2	radial distortion factor

$K\theta$	circumferential distortion factor
PLA	power lever angle
PS2	static pressure 0.457 m (17.992 in) ahead of inlet guide vanes, kPa (psia)
PT	total pressure, kPa (psia)
PTINF	free-stream total pressure, kPa (psia)
PT2	total pressure at the engine-face station, kPa (psia)
PT2AVG	average value of total pressure at engine face = $\sum_{n=1}^{n=35} \frac{PT2(n)}{35}$ kPa (psia)
PT2MAX	maximum value of total pressure at engine face, kPa (psia)
PT2MIN	minimum value of total pressure at engine face, kPa (psia)
RAMP3L	left inlet third ramp angle, deg
WAC	corrected engine airflow, $W2\sqrt{\theta t2}/\delta t2$, kg/sec (lb/sec)
WAC, percent	(WAC/98.43)100, where design corrected engine airflow = 98.43 kg/sec (217.0 lb/sec)
W2	engine airflow, kg/sec (lb/sec)
$\delta t2$	corrected average engine-face total pressure ratio
$\theta t2$	corrected average engine-face temperature ratio

Superscripts:

-	time-averaged data

DESCRIPTION OF APPARATUS

Flight test data were acquired using an F-15 aircraft (fig. 1) at the NASA Ames Research Center's Dryden Flight Research Facility. The F-15 aircraft is a high-performance, twin-engine fighter, capable of speeds to Mach 2.5. It has a high-mounted sweptback wing, twin vertical stabilizers, and a horizontal stabilator.

Propulsion System

Engine

The F100-PW-100 engine (fig. 2) is a low bypass-ratio (0.8), twin-spool, afterburning turbofan. The three-stage fan is driven by a two-stage, low-pressure turbine. The 10-stage, high-pressure compressor is driven by a two-stage, high-pressure turbine. The engine incorporates compressor inlet and rear compressor variable vanes to achieve high performance over a wide range of power settings. Continuously variable thrust augmentation is provided by a mixed-flow afterburner that is exhausted through a variable-area convergent-divergent nozzle. The F100 engine (Serial Number P680059) that had been previously calibrated in an altitude facility for thrust and airflow (ref. 4) was installed on the left side of the aircraft with the PS2 probe mounted on the hub.

Inlet

The F-15 aircraft has two side-mounted engine inlets which are of a two-dimensional horizontal ramp design (fig. 3). The inlets provide external compression with three ramps which feature a variable capture area by rotating the inlet about a transverse hinge point at the lower cowl lip. The ramps and bypass doors are automatically scheduled by the air inlet controller. For the distortion data presented in this report, the third inlet ramp was controlled manually in flight in order to vary the third ramp angle in increments.

DATA ACQUISITION AND REDUCTION

The general data parameters recorded for the test flights consisted of: the standard air data measurements; angles of attack and sideslip; and engine parameters such as rpm, throttle position, guide vane position, fuel flows, nozzle position, inlet variable geometry position, engine-face and turbine-discharge pressures. All steady-state data measurements were recorded digitally by a pulse code modulation system. Before the data were reduced, pretest and post-test zero corrections and power supply voltage corrections were made and applied to the raw data.

Engine Hub-Mounted PS2 Probe

Static pressure at the engine face was measured with four ports on a single probe 90° apart and manifolded to a single pressure line. The four ports on the probe were located 0.457 m (17.992 in) in front of the inlet guide vanes and the probe was mounted on the engine hub (figs. 4(a) to 4(c)). To increase measurement confidence, the single PS2 pressure line from the hub-mounted probe was connected to three pressure lines of equal length. The pressure from these lines was measured by three ±41368.5 N/m^2d (±6 psid) differential pressure transducers, the values of which were mathematically averaged and added to an absolute reference pressure (fig. 4(c)).

Engine-Face Total Pressure Probes

The total pressure array at the engine face, engine station 2, was mounted in the inlet guide vanes of the engine (figs. 4(a) and 4(b)). The array consisted of seven rakes, each having five total pressure probes located at the center of equal areas. To improve measurement accuracy, ±41368.5 N/m^2d (±6 psid) differential pressure transducers were used. Reference pressure for the differential pressure transducers was stabilized by the use of a reservoir tank that was pressurized by an inlet wall static and measured by a 0 to 344737.9 N/m^2a (0 to 50 psia) high-accuracy, digital, quartz transducer (see schematic of pressure instrumentation, fig. 4(c)). All of the transducers were in an environment that was temperature controlled.

Precision of Data

The instrumentation error sources are given in table 1. All of the error sources are predicted random errors. The errors shown include those associated with shifts because of temperature sensitivity, temperature zero shift, linearity and hysteresis, repeatability, and acceleration. The typical error in fan distortion as a function of pressure error was shown in reference 5 to be a normal 3-percent error in fan distortion for a 1-percent error in pressure.

ENGINE-FACE DATA REDUCTION

The engine-face pressure data taken in flight during conditions of high distortion was reduced and used in the calculation of several different parameters. The 35-probe, seven-rake array of total pressure probes at the engine face provided the data necessary to determine variations in pressure across the face of the engine and to arrive at the average value of total pressure (PT2AVG). Distortion parameters were calculated from the same data using analytical methods developed by Pratt & Whitney Aircraft Company for the F100 engine. The rake array consisted of seven rakes with five probes each, providing 35 measurements. The data reduction computer, however, required 40 measurements. A simple substitution technique using adjacent measurement values was employed to add five additional total pressure values; this completed the required set of 40 pressures. This set

was used to compute the values of distortion. When individual probes became inoperative, a replacement value was calculated and used in the distortion calculation.

For the steady-state data shown in this report, PT2AVG and PS2 pressure values were averaged over 5 to 10 sec to eliminate individual pressure fluctuations; these time-averaged pressures are labeled $\overline{PT2AVG}$ and $\overline{PS2}$. However, total pressure values used in the calculation of fan distortion factor (KA2), circumferential distortion factor (Kθ), and radial distortion factor (KRA2) were not averaged over time, but were determined from one time frame only. The equations used in the calculation of the distortion descriptors are given in reference 6 and shown in table 2. These distortion factors consist of the fan circumferential Kθ, the fan radial KRA2, and the overall fan distortion factor KA2. The radial distortion weighting factor (b, ref. 6 and fig. 5) was developed specifically for the F100-PW-100 turbofan engine.

The distortion factor DTMM consists of the conventional maximum-minus-minimum-over-average total pressure ratio (PT2MAX - PT2MIN)/PT2AVG). The equation for DTMM is also given in table 2. Values of DTMM were averaged over the same 5 to 10 sec as PT2AVG and PS2.

TEST CONDITIONS AND PROCEDURES

All of the distortion data were taken at stabilized Mach numbers of 0.8 and 0.9 and at altitudes of 9140 and 12,190 m (30,000 and 40,000 ft, see table 3). The left inlet third ramp was driven in steps from the full-up position to the full-down position or until the engine stalled (fig. 6), while the right engine was used to maintain speed and altitude. Each new ramp position, or step, was held for approximately 20 sec, allowing all pressure ratios and airflows to stabilize while holding power lever angle (PLA) constant. Only run 2 was performed at a PLA setting below intermediate power; hence, run 2-corrected engine airflow was lower than the maximum corrected airflow that was available to the engine during the other three distortion runs.

RESULTS AND DISCUSSION

Low Distortion

The PS2 static pressure probe was tested in an altitude facility on an F100 engine and in flight in the inlet of an F-15 airplane. Steady-state reduced power data obtained at Mach 0.9 and an altitude of 12,190 m (40,000 ft) were compared with data obtained from a different engine in an altitude facility. The data from flight and the altitude facility compared PT2AVG/PS2 pressure ratio with corrected engine airflow (WAC, percent) and showed that no measurable shift in PT2AVG/PS2 occurred with changing airflow (see fig. 7 and ref. 2). Other flight test conditions, including Mach number excursion and maximum load factor turns, also showed good agreement with previous altitude facility test results.

Induced Distortion

Increased levels of distortion in the inlet were induced during flight test by lowering the inlet third ramp in a series of steps (see figs. 3 and 6). With increasing third ramp angle, the inlet throat area was reduced, causing the inlet throat Mach number to increase. When this happened, the $\overline{PT2AVG}/\overline{PS2}$ pressure ratio (engine-face Mach number) gradually increased until engine stall occurred. The distortion factors KA2, Kθ, and $\overline{DTMM}$ also increased with increasing third ramp angle (figs. 8(a) to 8(d)). The radial distortion factor KRA2 changed very little. Since the fan distortion factor KA2 = f(Kθ + b(KRA2)),

the influence of Kθ and KRA2 could be seen in KA2. When the distortion factor data from each of the four ramp excursions were combined on one plot (figs. 9(a) to 9(d)), the repeatable nature of each of the distortion factors became evident: KA2 and Kθ showed large values of distortion with increasing third ramp angle (figs. 9(a) and 9(b)); KRA2 showed a change in slope around 18° third ramp angle (fig. 9(c)); and $\overline{DTMM}$ did not vary significantly with third ramp angle (fig. 9(d)).

Engine-Face Distortion Maps

The engine-face distortion maps (figs. 10(a) to 10(f)) show increasing pressure distortion as the inlet third ramp angle is increased. The pressure patterns change from the relatively symmetrical shapes of low distortion to the classical 180° distortion patterns seen just before engine stall (depicted in fig. 10(f)). These 180° distortion patterns have relatively large pressure gradients across the engine face with high pressure on the inboard side and low pressure on the outboard side. The series of maps presented in figure 10(a) only represent every other data point evaluated for run 1; however, the distortion patterns seen in this series of maps were typical for all of the distortion changes caused by the ramp excursions. These distortion maps are a graphical presentation of the pressure distributions at the engine face and illustrate the calculated values of the distortion factors Kθ and KRA2 when showing whether the increase in distortion is radial or circumferential. The calculated distortion factors Kθ, KA2, KRA2, and DTMM, however, provide numerical values that can be better evaluated and compared.

Distortion Correlated With $\overline{PT2AVG}/\overline{PS2}$

When the pressure ratio $\overline{PT2AVG}/\overline{PS2}$ is compared with distortion factors Kθ, KA2, KRA2, and $\overline{DTMM}$, good correlation exists for all factors except for the radial distortion factor, KRA2 (see figs. 11(a) to 11(d)). The circumferential distortion factor Kθ, shown in figure 11(a), exhibits a good linear correlation with $\overline{PT2AVG}/\overline{PS2}$ for all four tests. The effects of free-stream Mach number, altitude, or airflow differences are not evident in the data. The $\overline{DTMM}$ distortion factor also shows good correlation with no apparent effect of free-stream Mach number, altitude, or airflow differences (fig. 11(b)). The radial distortion factor KRA2 (fig. 11(c)) does not increase to a large value, indicating that only a minimal amount of radial distortion could be attributed to the closing down of the inlet third ramp. Therefore, the data from figures 11(a) and 11(c) show that for these conditions, the predominant distortion is circumferential and not radial.

The distortion factor KA2 was developed by the engine manufacturer specifically for the F100 engine. This factor consists of the sum of Kθ, which correlates well with $\overline{PT2}/\overline{PS2}$, and KRA2 multiplied by the weighting factor b, which is a function of airflow (fig. 5). This can cause KA2 to vary with airflow as evidenced in run 2 of figure 11(d). When airflow conditions are constant, KA2 correlates very well with $\overline{PT2AVG}/\overline{PS2}$ pressure ratio. The distortion value KA2 increases rapidly prior to engine stall.

In the preceding sections, it has been shown that during conditions of high distortion at the engine face, near-linear relationships exist for certain distortion parameters. In particular, KA2, Kθ, and $\overline{DTMM}$ correlate very well with the pressure ratio $\overline{PT2AVG}/\overline{PS2}$ for the flight conditions tested. These relationships confirm that the PS2 pressure probe can be useful as an engine control parameter as shown in reference 3.

CONCLUSIONS

A hub-mounted probe to measure engine-face static pressure was evaluated in an F-15 aircraft flying at subsonic speeds. The following are concluded:

1. For low-distortion conditions, the ratio of engine-face total pressure to static pressure agreed well with previous altitude facility data.

2. During tests in which the inlet throat area was reduced, large amounts of circumferential distortion occurred, but only small amounts of radial distortion occurred.

3. For high-distortion conditions, the ratio of engine-face total pressure to static pressure correlated well with the circumferential distortion factor $K\theta$, the fan distortion factor KA2, and the maximum-minus-minimum-over-average distortion factor DTMM.

Ames Research Center
Dryden Flight Research Facility
National Aeronautics and Space Administration
Edwards, California, May 2, 1983

REFERENCES

1. Foote, C. H.: Final Report Data Analysis of PT/PS Noseboom Probe Testing on F100 Engine P680072 at NASA Lewis Research Center. NASA CR-159816, 1980.

2. Foote, C. H.; and Jaekel, R. J.: Flight Evaluation of an Engine Static Pressure Noseprobe in an F-15 Airplane. NASA CR-163109, 1981.

3. Digital Electronic Engine Control (DEEC) Flight Evaluation in an F-15 Airplane. NASA CP-2298, 1984.

4. Biesiadny, Thomas J.; Lee, Douglas; and Rodriguez, Jose R.: Airflow and Thrust Calibration of an F100 Engine, S/N P680059, at Selected Flight Conditions. NASA TP-1069, 1978.

5. Farr, A. P.; and Schumacher, G. A.: System for Evaluation of F-15 Inlet Dynamic Distortion. McDonnell Aircraft Co., McAIR 72-043, Sept. 1972.

6. Stevens, C. H.; Spong, E. D.; and Hammock, M. S.: F-15 Inlet/Engine Test Techniques and Distortion Methodologies Studies, Volume 1 - Technical Discussion. NASA CR-144866, 1978.

TABLE 1. — PARAMETER RANGE AND ACCURACY

Parameter	Units	Range	Accuracy	Resolution	Rms*
PT2	N/m^2d (psid)	41368.5 (6)	±157.2 (±0.0228)	±413.7 (±0.06)	±391.6 (±0.0568)
PS2 (sum of 3)	N/m^2d (psid)	41368.5 (6)	±111.0 (±0.0161)	±193.1 (±0.028)	±375.1 (±0.0544)
Reference pressure (digital quartz)	N/m^2 (psia)	0 to 344737.9 (0 to 50)	±137.9 (±0.02)	---	---
PCM error	N/m^2 (psia)	- - -	330.9 (0.048)	---	---

*Root mean square = $\left[(\text{accuracy})^2 + (\text{reference pressure})^2 + (\text{PCM error})^2\right]^{1/2}$

TABLE 2. — EQUATIONS USED IN CALCULATION OF DISTORTION

(a) Fan circumferential distortion descriptor

$$K\Theta = \frac{\sum_{Ring=1}^{J} \left[\left(\frac{aN}{N^2}\right)_{max}\right]_{ring} \times \frac{1}{D_{ring}}}{\left(\frac{q}{PT2}\right)_{ref} \sum_{Ring=1}^{J} \frac{1}{D_{ring}}}$$

where

J = number of rings (probes per leg)

D = ring diameter

$\left(\frac{q}{PT2}\right)_{ref}$ = reference value of engine-face dynamic pressure head; function of engine-face Mach number

$aN = \sqrt{aN^2 + bN^2}$, $N = 1,2,3,4$

where

$$aN = \frac{\Delta\theta}{180} \sum_{K=1}^{K} \frac{\frac{PT2(K\Delta\theta)}{PT0}}{\frac{\overline{PT2}}{PT0}} \cos(NK\Delta\theta)$$

$$bN = \frac{\Delta\theta}{180} \sum_{K=1}^{K} \frac{\frac{PT2(K\Delta\theta)}{PT0}}{\frac{\overline{PT2}}{PT0}} \sin(NK\Delta\theta)$$

and

$\frac{PT2(K\Delta\theta)}{PT0}$ = local recovery at angle $K\Delta\theta$

$\left(\frac{\overline{PT2}}{PT0}\right)$ = face average recovery

K = number of rake legs

$\Delta\theta$ = angular distance between rake legs, deg

$\left(\frac{aN}{N^2}\right)_{max}$ = maximum value for the four Fourier coefficients calculated (normally A1)

TABLE 2. — Concluded

(b) Fan radial distortion descriptor

$$KRA2 = \frac{\sum_{Ring=1}^{J} \left(\frac{\Delta PT2}{PT2}\right)_{ring} \frac{1}{D_{ring}}}{\left(\frac{q}{PT2}\right)_{ref} \sum \frac{1}{D_{ring}}}$$

with

$$\left(\frac{\Delta PT2}{PT2}\right)_{ring} = \left| \frac{\left(\frac{PT2^*}{PT0}\right)}{\frac{\overline{PT2}}{PT0}} - \frac{PT2^*_{base}}{\overline{PT2}} \right| \frac{\overline{PT2}}{PT2^*_{base}}$$

where

$\frac{PT2^*}{PT0}$ = ring average recovery

$\frac{PT2^*_{base}}{\overline{PT2}}$ = reference radial profile; function of corrected engine airflow

b = radial distortion weighting factor; function of corrected engine airflow

PT0 = free-stream total pressure

(c) Fan distortion descriptor

$$KA2 = K\theta + b(KRA2)$$

(d) Maximum-minus-minimum-over-average distortion

$$DTMM = \frac{PT2MAX - PT2MIN}{PT2AVG}$$

TABLE 3. — SUMMARY OF RUN CONDITIONS

Run	Mach number	Altitude, m (ft)	Cowl angle, deg	WAC, percent	Angle of attack, deg
1	0.9	12,190 (40,000)	8.5 to 7.7	105.5 to 106.5	2.5
2	0.9	9,140 (30,000)	7.3 to 6.7	102.0 to 103.0	1.2
3	0.8	12,190 (40,000)	5.7 to 6.1	105.5 to 107.5	3.6
4	0.8	9,140 (30,000)	4.4	105.5 to 107.0	2.0

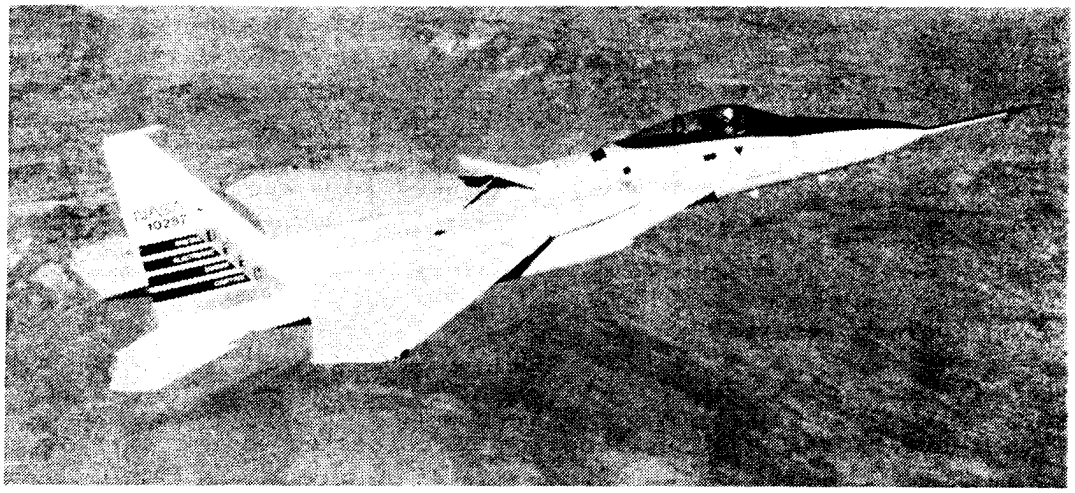

ECN 17701

Figure 1. F-15 airplane.

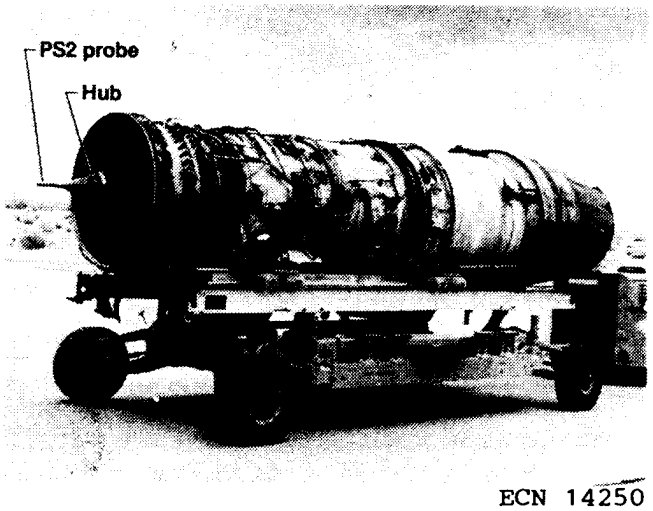

ECN 14250

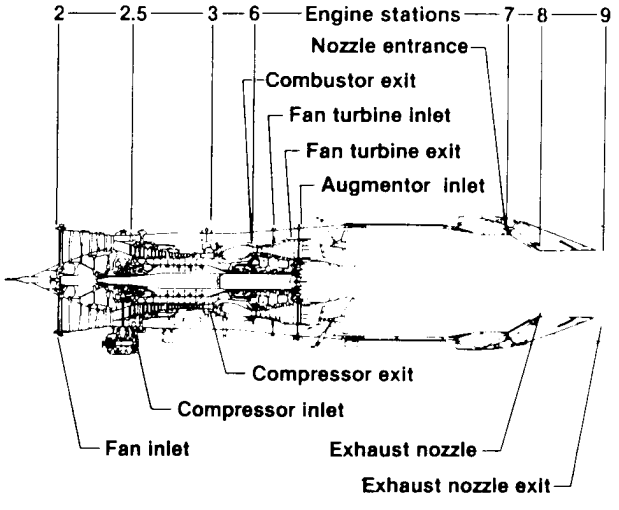

(a) Engine, serial number P680059. *(b) Schematic of engine and station.*

Figure 2. F100-PW-100 engine with PS2 probe.

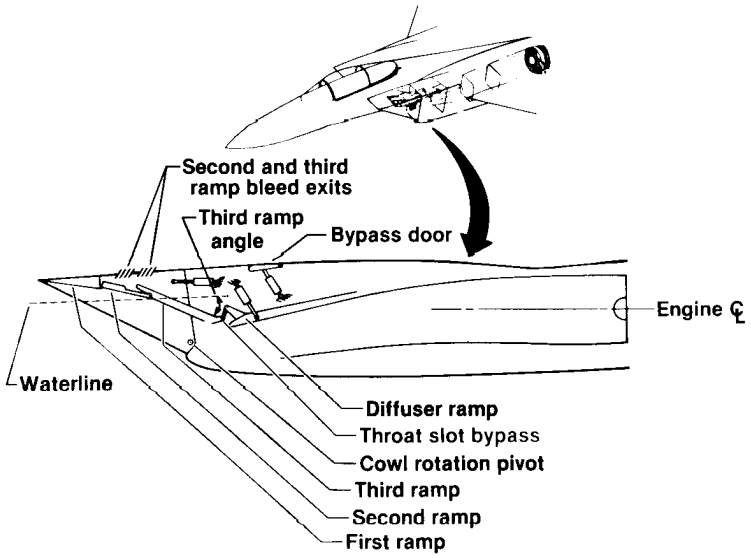

Figure 3. F-15 engine inlet.

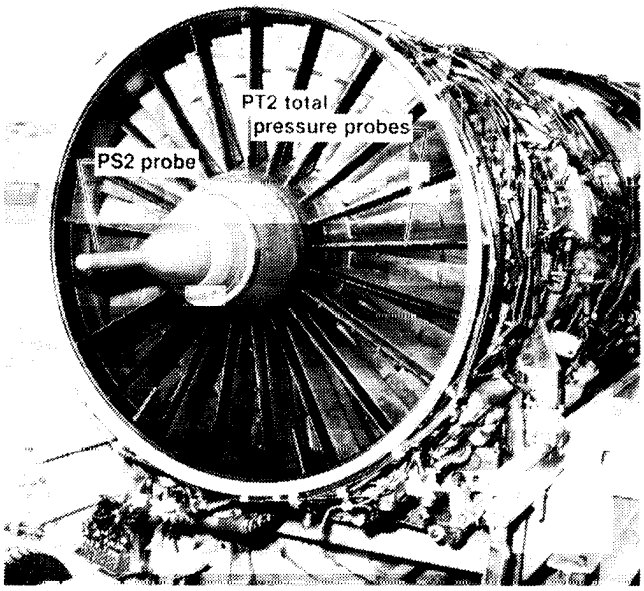

ECN 14251

(a) PS2 and PT2 probes at the engine face.

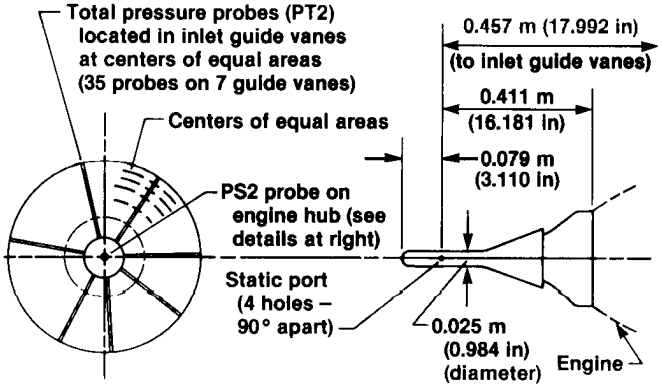

(b) Engine-face pressure instrumentation.

Figure 4. F100-PW-100 engine face.

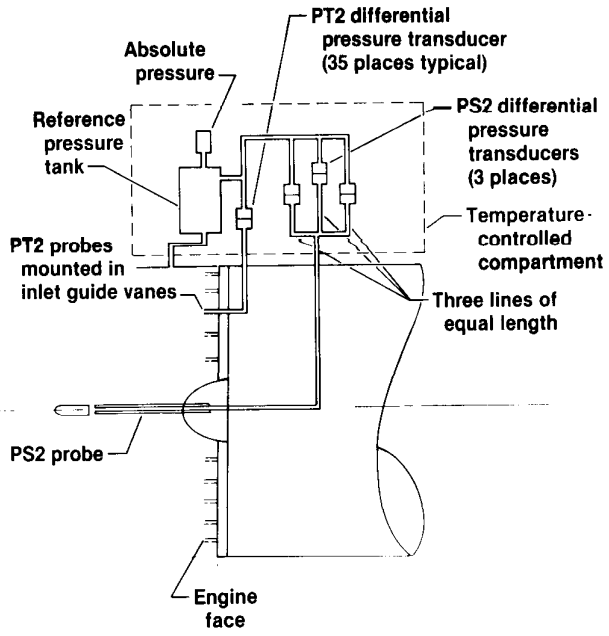

(c) PS2 and PT2 pressure measurement system.

Figure 4. Concluded.

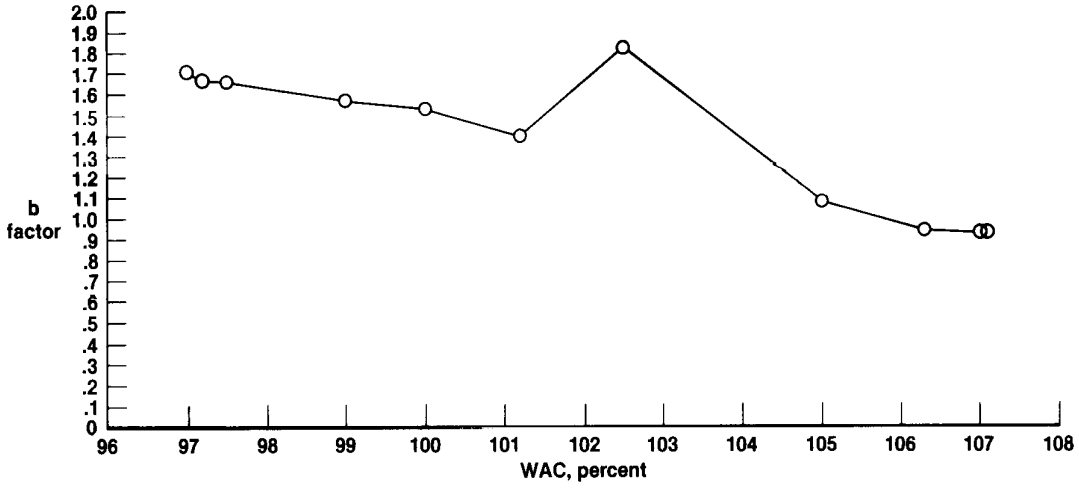

Figure 5. Relationship of b weighting factor as a function of corrected engine airflow.

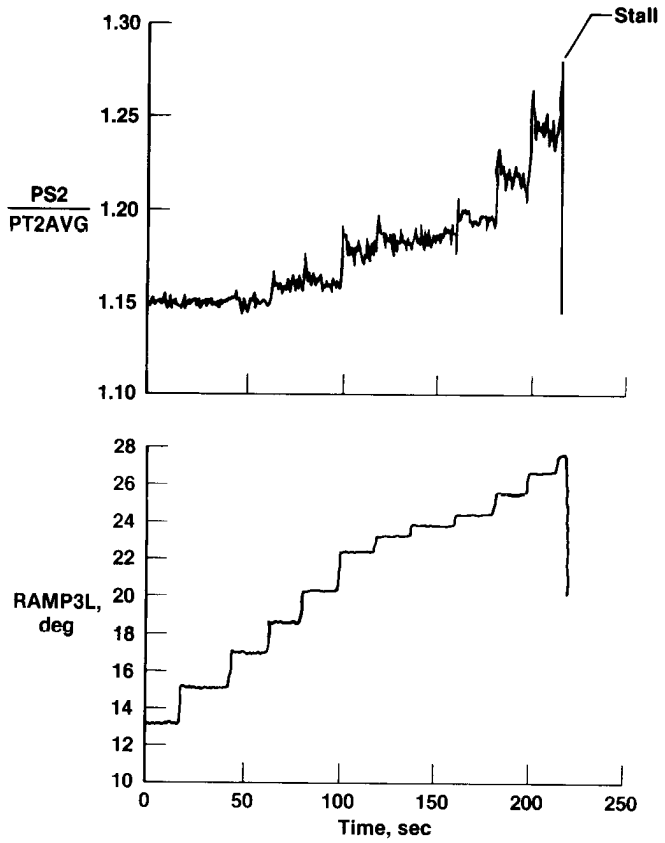

Figure 6. Time history of PT2/PS2 distortion increase as inlet third ramp angle is increased.

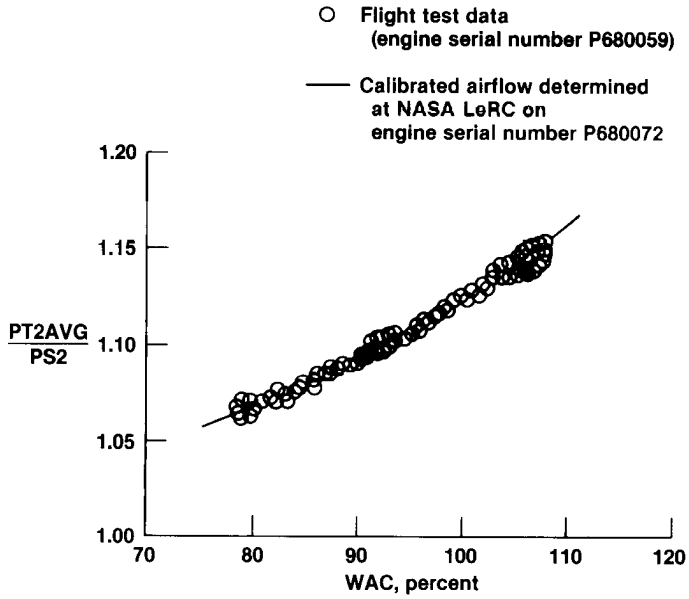

Figure 7. Variation of engine-face total probe static pressure ratio with percent corrected airflow.

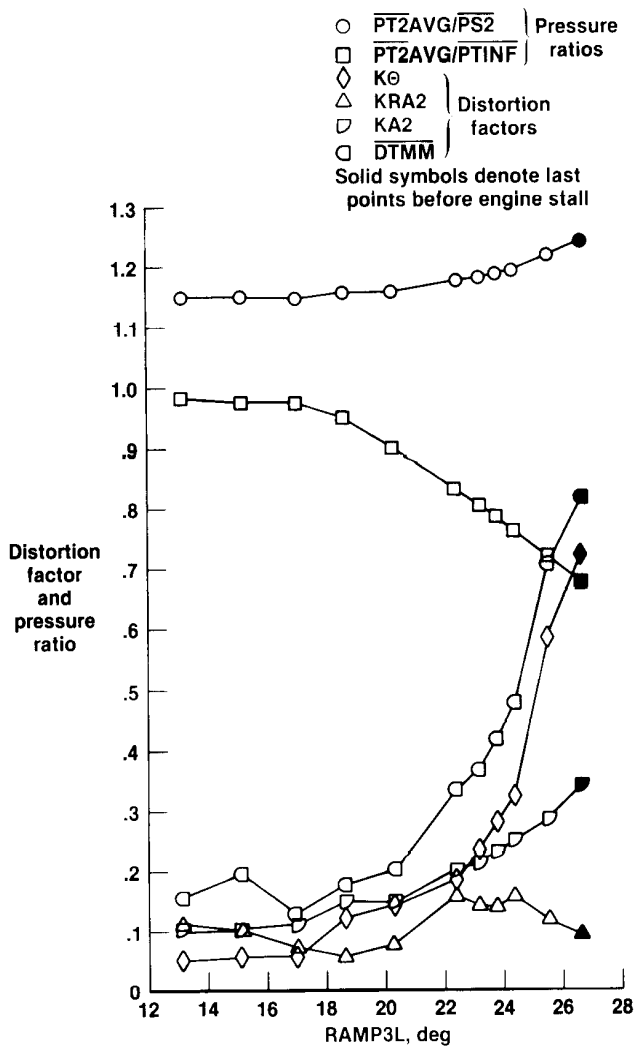

(a) Run 1. Mach 0.9; altitude = 12,190 m (40,000 ft); WAC, percent = 105 to 107.

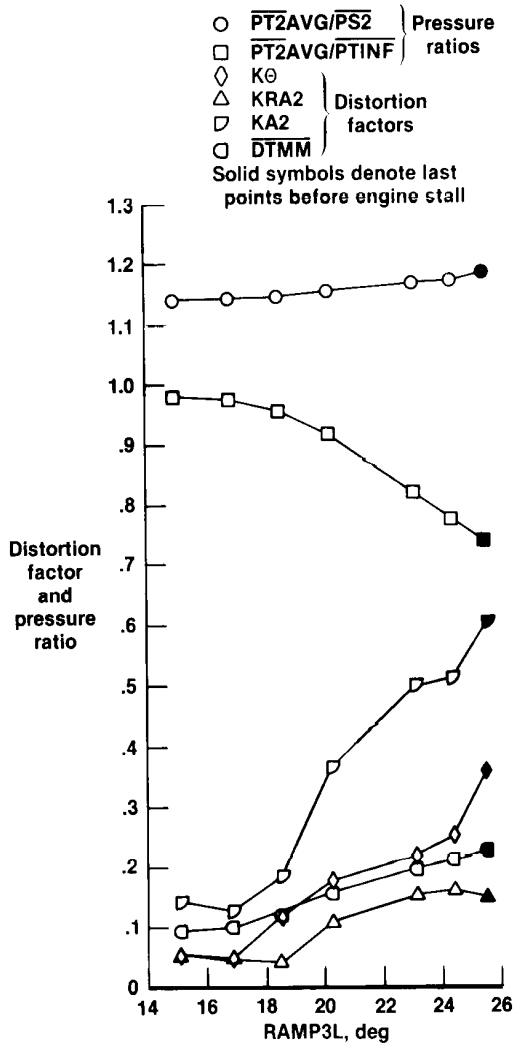

(b) Run 2. Mach 0.9; altitude = 9140 m (30,000 ft); WAC, percent = 101 to 103.

Figure 8. Distortion factor and pressure ratio as a function of inlet third ramp angle.

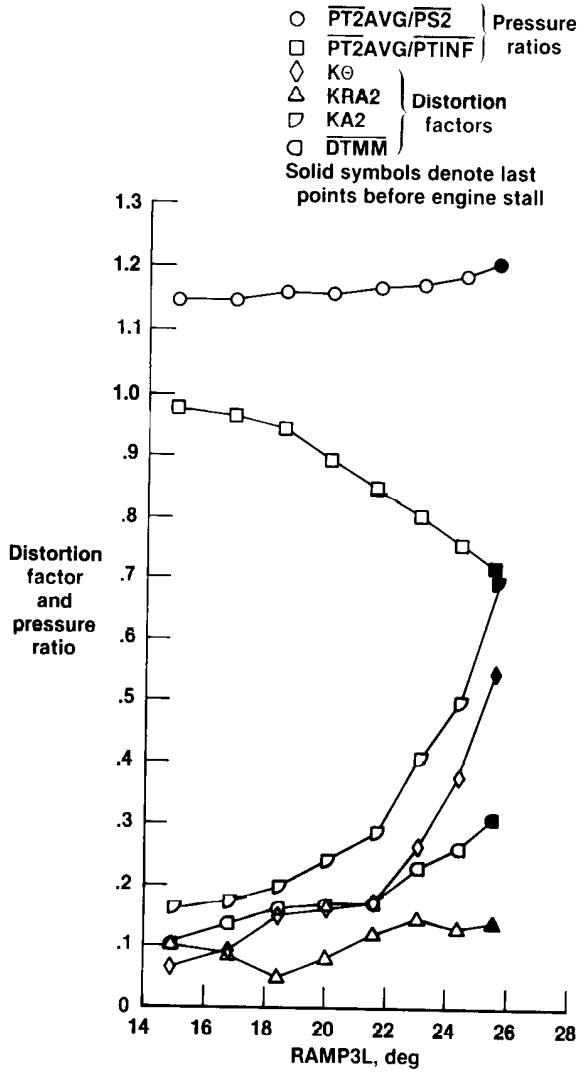

(c) Run 3. Mach 0.8; altitude = 12,190 m (40,000 ft); WAC, percent = 105 to 107.

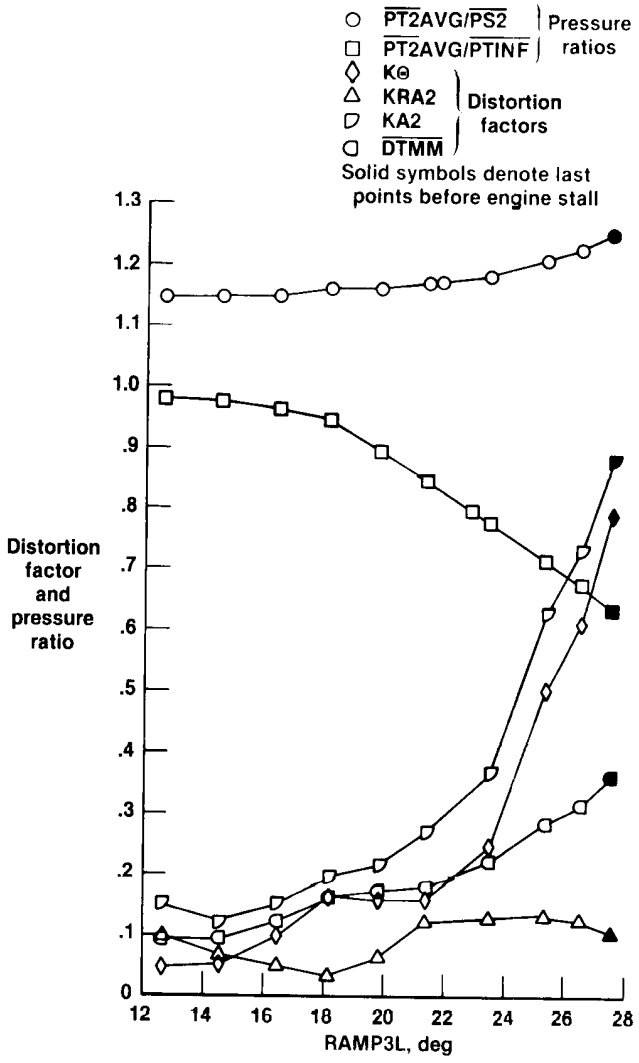

(d) Run 4. Mach 0.8; altitude = 9140 m (30,000 ft); WAC, percent = 105 to 107.

Figure 8. Concluded.

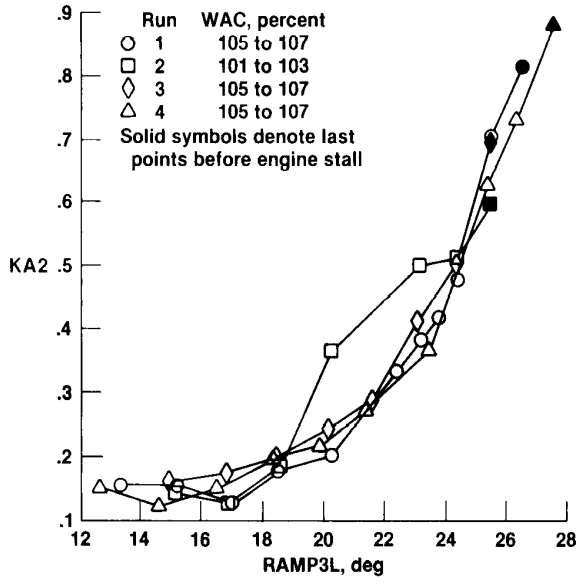

(a) KA2 distortion factor.

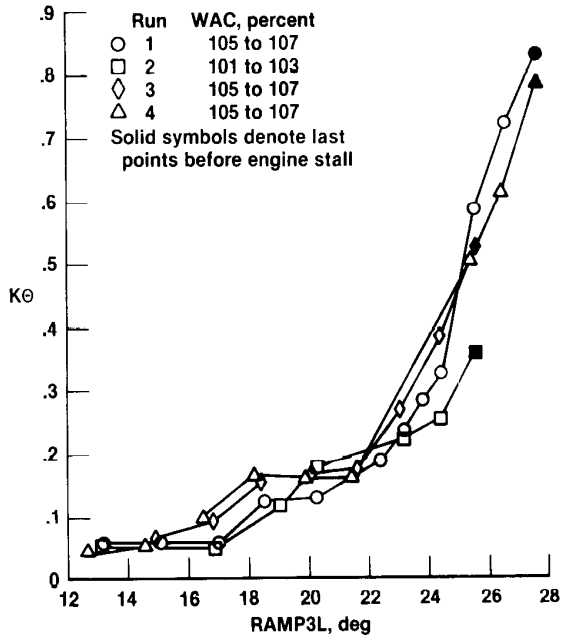

(b) KΘ distortion factor.

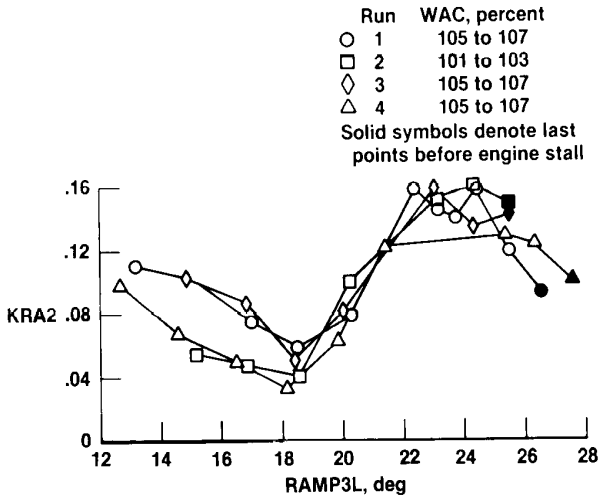

(c) KRA2 distortion factor.

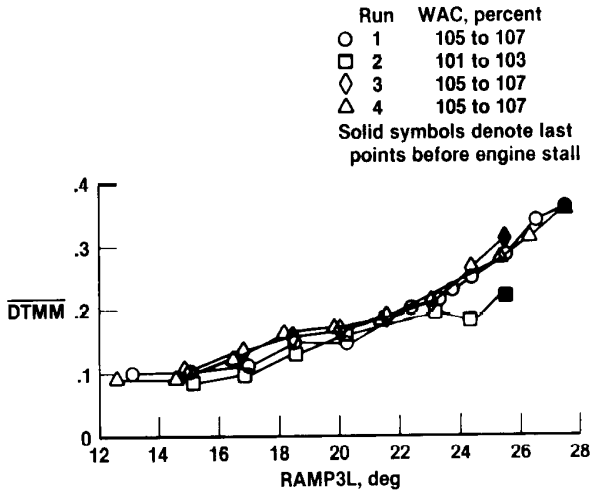

(d) DTMM distortion factor.

Figure 9. Distortion factors as a function of inlet third ramp angle.

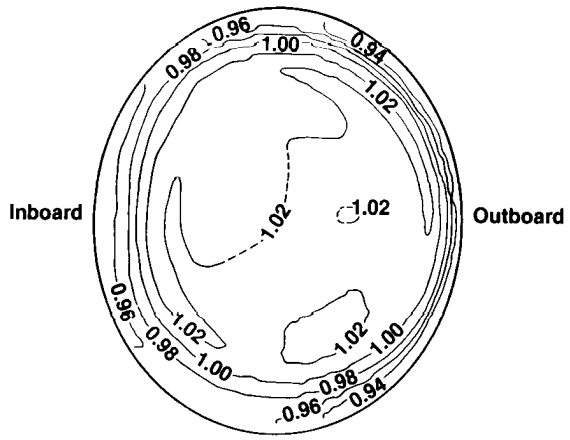

(a) Ramp angle = 15.1°;
PT2AVG = 30.25 kPa;
KA2 = 0.295;
Kθ = 0.0584;
KRA2 = 0.1024;
DTMM = 0.01048; and
WAC, percent = 106.64.

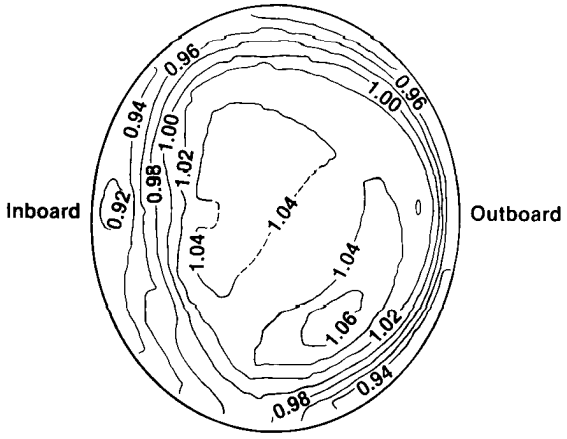

(b) Ramp angle = 18.5°;
PT2AVG = 29.16 kPa;
KA2 = 0.26054;
Kθ = 0.1222;
KRA2 = 0.0596;
DTMM = 0.1504; and
WAC, percent = 106.80.

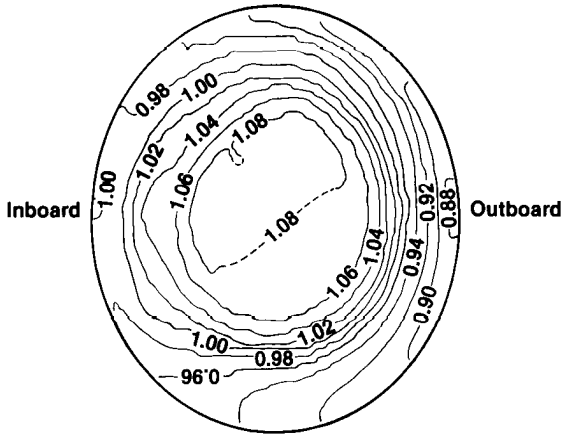

(c) Ramp angle = 22.4°;
PT2AVG = 26.00 kPa;
KA2 = 0.5508;
Kθ = 0.1861;
KRA2 = 0.1589;
DTMM = 0.2029; and
WAC, percent = 106.3.

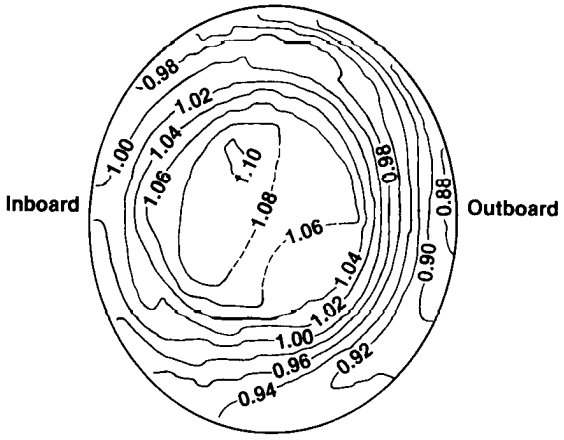

(d) Ramp angle = 23.8°;
PT2AVG = 24.66 kPa;
KA2 = 0.6042;
Kθ = 0.2820;
KRA2 = 0.1401;
DTMM = 0.2320; and
WAC, percent = 105.94.

Figure 10. Engine-face pressure contour map, Run 1. Mach 0.9; altitude = 12,190 m (40,000 ft).

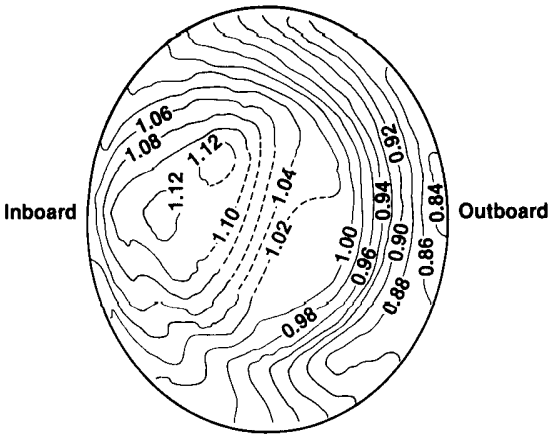

(e) Ramp angle = 25.5°;
PT2AVG = 22.48 kPa;
KA2 = 0.8634;
Kθ = 0.586;
KRA2 = 0.1198;
DTMM = 0.2871; and
WAC, percent = 105.80.

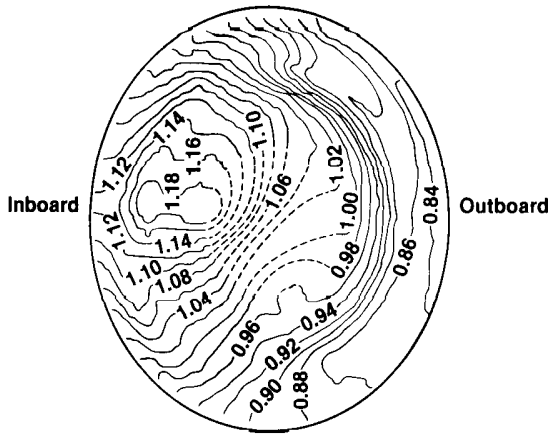

(f) Ramp angle = 27.5°;
PT2AVG = 20.37 kPa;
KA2 = 1.156;
Kθ = 0.820;
KRA2 = 0.1306;
DTMM = 0.3643; and
WAC, percent = 105.35.

Figure 10. Concluded.

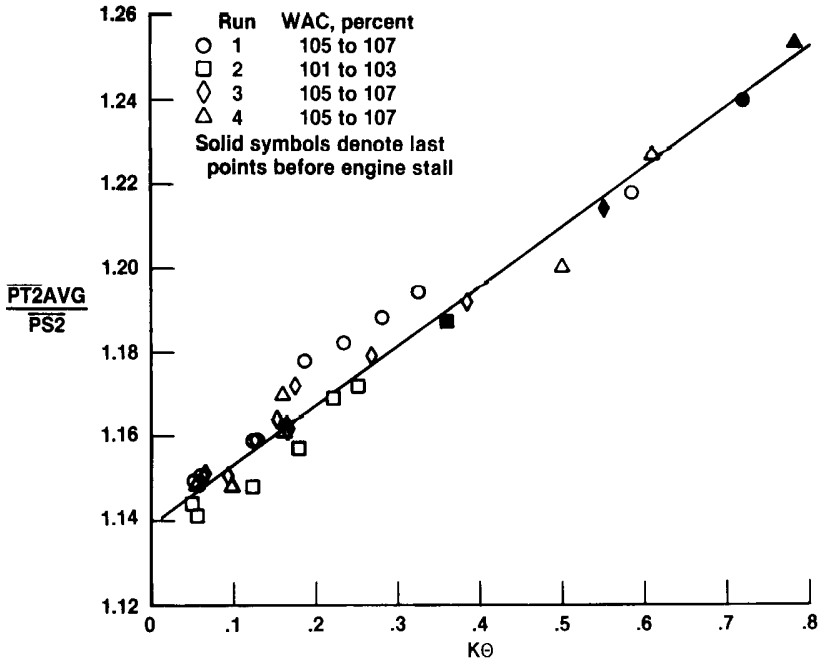

(a) Kθ distortion factor.

Figure 11. Ratio of inlet total to static pressure as a function of distortion factor.

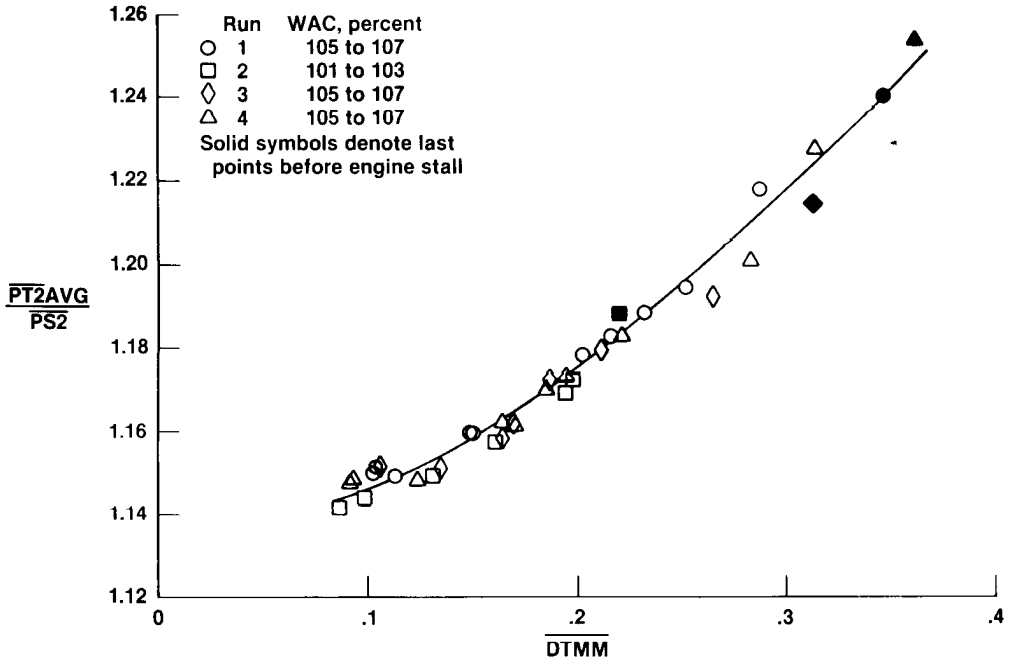

(b) DTMM distortion factor.

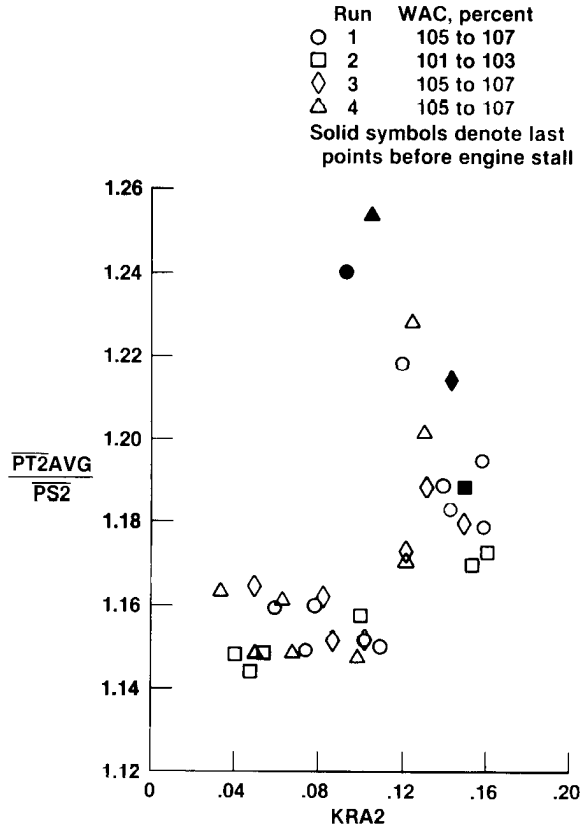

(c) KRA2 distortion factor.

Figure 11. Continued.

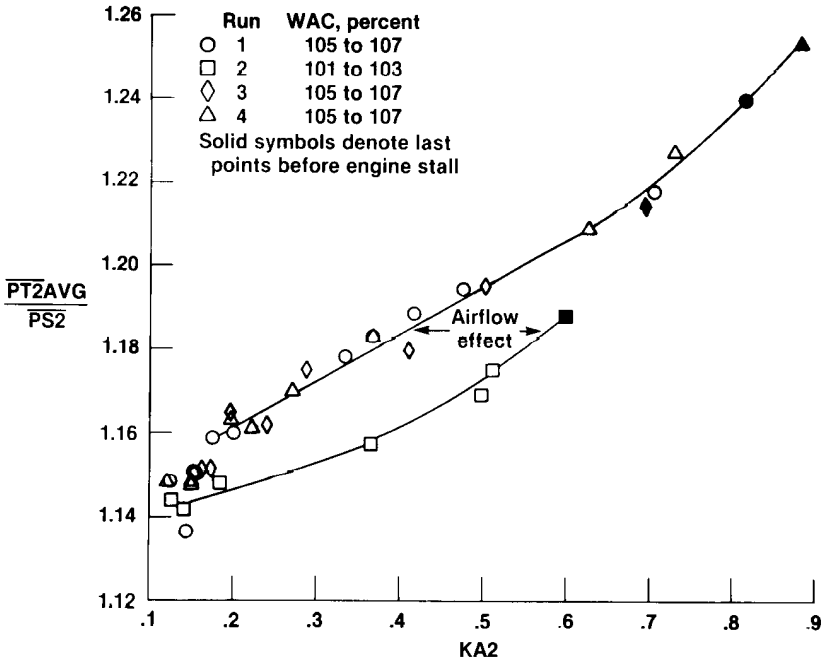

(d) KA2 distortion factor.

Figure 11. Concluded.

1. Report No.	2. Government Accession No.	3. Recipient's Catalog No.
NASA TP-2411		

4. Title and Subtitle	5. Report Date
Effects of Inlet Distortion on a Static Pressure Probe Mounted on the Engine Hub in an F-15 Airplane	April 1985
	6. Performing Organization Code

7. Author(s)	8. Performing Organization Report No.
Donald L. Hughes, Lawrence P. Myers, and Karen G. Mackall	H-1182
	10. Work Unit No.

9. Performing Organization Name and Address	11. Contract or Grant No.
NASA Ames Research Center Dryden Flight Research Facility P.O. Box 273 Edwards, California 93523	
	13. Type of Report and Period Covered
12. Sponsoring Agency Name and Address	Technical Paper
National Aeronautics and Space Administration Washington, D.C. 20546	14. Sponsoring Agency Code RTOP 533-02-21

15. Supplementary Notes

16. Abstract

An inlet static pressure (PS2) probe was mounted on the hub of an F100 engine in an F-15 airplane. Flight test results showed that for low distortion conditions, the ratio of engine-face total pressure to static pressure agreed well with previous altitude facility data. Off-schedule operation of the inlet third ramp angle caused increased distortion of the inlet airflow during steady-state flight conditions. Data are shown for inlet third ramp excursions leading to engine stall. The relationships of inlet face total to static pressure ratio as a function of several distortion descriptors are also described.

17. Key Words (Suggested by Author(s))	18. Distribution Statement
Inlet distortion Static pressure (PS2)	Unclassified - Unlimited Subject Category 07

19. Security Classif. (of this report)	20. Security Classif. (of this page)	21. No. of Pages	22. Price
Unclassified	Unclassified	21	A02

For sale by the National Technical Information Service, Springfield, Virginia 22161.

NASA-Langley, 1985